06.1;12.1

Production of dispersed metal-matrix multicomponent composites Al/Cu−Mg−W−C in the arc discharge plasma

© D.S. Nikitin[1], A. Nassyrbayev[1], A.I. Tsimmerman[1], I.I. Shanenkov[1,2], A.A. Sivkov[1,3]

[1] Tomsk Polytechnic University, Tomsk, Russia
[2] University of Tyumen, Tyumen, Russia
[3] Jilin University, Changchun, Jilin, China
E-mail: nikitindmsr@yandex.ru

Received February 9, 2024
Revised March 29, 2024
Accepted April 4, 2024

The Al/Cu-Mg-W-C composite was synthesized in the plasma of an arc discharge generated by a coaxial magnetoplasma accelerator with aluminum electrodes. The dispersed product contains nanoparticles of the unique crystalline phase of cubic tungsten carbide WC_{1-x}, hexagonal modification W_2C, and copper and magnesium spinels. The synthesized material is suitable for producing on its base bulk metal-matrix products reinforced with superhard compounds.

Keywords: composites, powders, plasma, arc discharge.

DOI: 10.61011/TPL.2024.07.58737.19885

Aluminum and its alloys are among the materials most commonly used in various constructional and functional applications. Regardless of the benefits of using component parts made from aluminum, manufacturers of a variety of commercial products strive to develop next-generation materials expected to compete in functionality with conventional ones. The most promising way is, first of all, to use various metal-matrix composites [1]. For instance, aluminum-matrix-based composite materials combine excellent ductility, corrosion resistance, aluminum recyclability and formability and, in addition, high rigidity, strength, hardness and wear resistance of the ceramic reinforcement component [2].

One of the trends in works devoted to metal-matrix composites is reinforcement with nanodispersed particles, as well as production of nanocomposites in general [3]. As such components for aluminum, there are commonly used carbon structures (nanofibers, carbon nanotubes and graphene nanoplates), as well as carbides (SiC, TiC, B_4C, etc.) [4–6]. One of the most promising reinforcing materials seems to be nanodispersed tungsten carbide that, being applied, improves the compositesẃear resistance and tribological characteristics, as well as high-temperature mechanical and corrosion properties [7,8]. General problems faced in nanocomposites fabrication and nanoreinforcement are the difficulty of providing a uniform distribution of the reinforcing component and its incompatibility with the metal matrix, which restrict employing such materials in various fields of engineering [9]. Another innovative strategy for developing up-to-date metal-matrix composites is multi-component (including high-entropy compounds) [10] and hybrid [11] reinforcement, when adding various reinforcing components to the metal matrix induces a number of synergistic effects promoting improvement of mechanical and functional characteristics.

One of the ways to create the Al/W−C metal-matrix composites with the possibility of implementing modern strategies for their development is synthesis in a high-speed arc discharge plasma jet generated by a coaxial magnetoplasma accelerator. Previously there were conducted experiments involving electrode systems made from aluminum and other metals without introducing other substances into the channel of plasma structure formation [12]. We have demonstrated the possibility of synthesizing nonstoichiometric cubic tungsten carbide WC_{1-x} for a graphite electrode system [13]. This crystalline phase is metastable and thermally sensitive because of phase transitions taking place at temperatures above 1000°C; this is why it can be preserved in the bulk form being included in metal-matrix composites. In this case, the preferable way to obtain the Al/WC_{1-x} composite is the *in situ* approach implying that synthesis of WC_{1-x} proceeds if a dispersed material to be used as a charge for subsequent fabrication of finished products (e.g. by sintering) is formed simultaneously.

To obtain the dispersed composite, a coaxial magnetoplasma accelerator with aluminum electrodes (alloy D1) was used. The material chemical composition is given in Table 1. As the table shows, the most significant impurities in the aluminum alloy are Cu and Mg. Taking into account that the metal matrix is created using this alloy, the final composite may be represented as Al/Cu−Mg−WC_{1-x}. The last composite component (cubic tungsten carbide) is formed by putting into the plasma structure formation channel the tungsten/carbon mixture in the 0.171:0.031 g ratio. As a power supply for the coaxial magnetoplasma accelerator, a capacitive energy-storage device was used. At the storage capacity of $C = 14.4$ mF and charging voltage of

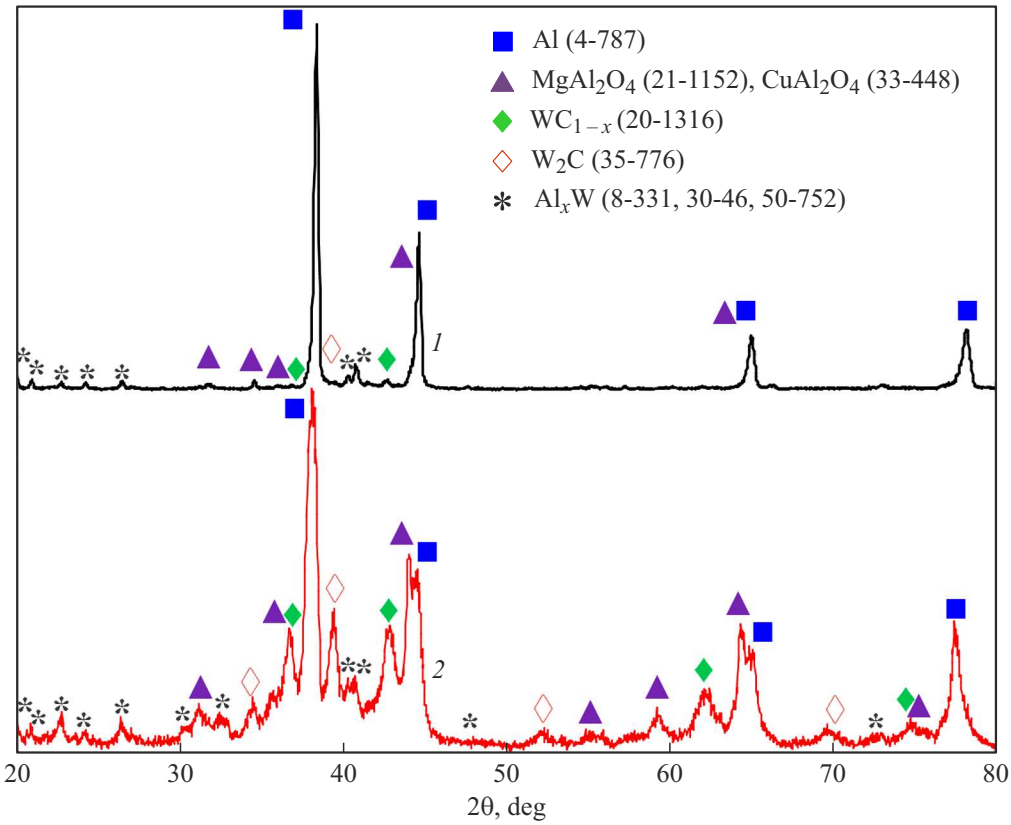

Figure 1. X-ray diffraction patterns of synthesized products from the main (*1*) and buffer (*2*) chambers.

Table 1. Elemental composition (in mass%) of the aluminum alloy for the accelerator electrodes

Al	Cu	Mg	Mn	Si	Ti	Zn	Fe	Cr
94.7	3.5	0.8	0.4	0.2	0.1	0.1	0.1	0.1

Table 2. Estimated contents of the crystalline phases contained in the main-chamber and buffer-chamber synthesis products.

Chamber	Content, mass%			
	Al	$MgAl_2O_4$+$CuAl_2O_4$	WC_{1-x}+W_2C	Al_xW
Main	89.9	2.0	3.0	5.1
Buffer	53.4	26.0	17.2	3.4

$U = 2$ kV, the released energy was 23.9 kJ. The plasma jet entered the main chamber connected to the low-pressure buffer chamber for pumping out the highly dispersed fraction of the suspended synthesized product.

As a result of plasmadynamic synthesis under the above-mentioned conditions, dispersed materials were produced; their phase compositions were studied by X-ray diffractometry (Shimadzu XRD7000, CuK_α radiation). Fig. 1 presents X-ray diffraction patterns of the synthesized products from the main and buffer chambers. The main common feature of the presented diffraction patterns is the predominant content of the aluminum crystalline phase arising as a result of electric erosion of the accelerator electrode system. Results of the estimative (quantitative) X-ray phase analysis (Table 2) performed by the Rietveld method using the PDF2+ database and PowderCell 2.4 software package showed that the aluminum content in the buffer-chamber product (~ 53 mass%) is less than that in the main-chamber (~ 90 mass%). In addition, the buffer-chamber product is characterized by much broader diffraction reflections and significantly smaller coherent-scattering region (11 and 72 nm for aluminum from the buffer and main chambers, respectively), which confirms its high dispersion. Broadening of the X-ray maxima is obvious not only for aluminum, but also for other phases, i. e. all the buffer-chamber product is nanodispersed.

Besides aluminum, other crystalline phases also exist in the synthesized products. First, the material contains compounds whose formation is explained by the composition of aluminum alloy used to fabricate the electrode system. These are spinels $MgAl_2O_4$ and $CuAl_2O_4$ whose formation is caused, on the one hand, by the presence of copper and magnesium in aluminum alloy D1, and, on the other hand, by the presence of an oxide film consisting predominantly of magnesium and copper oxides [14]. Just this film with its constituent oxides of aluminum, magnesium and copper

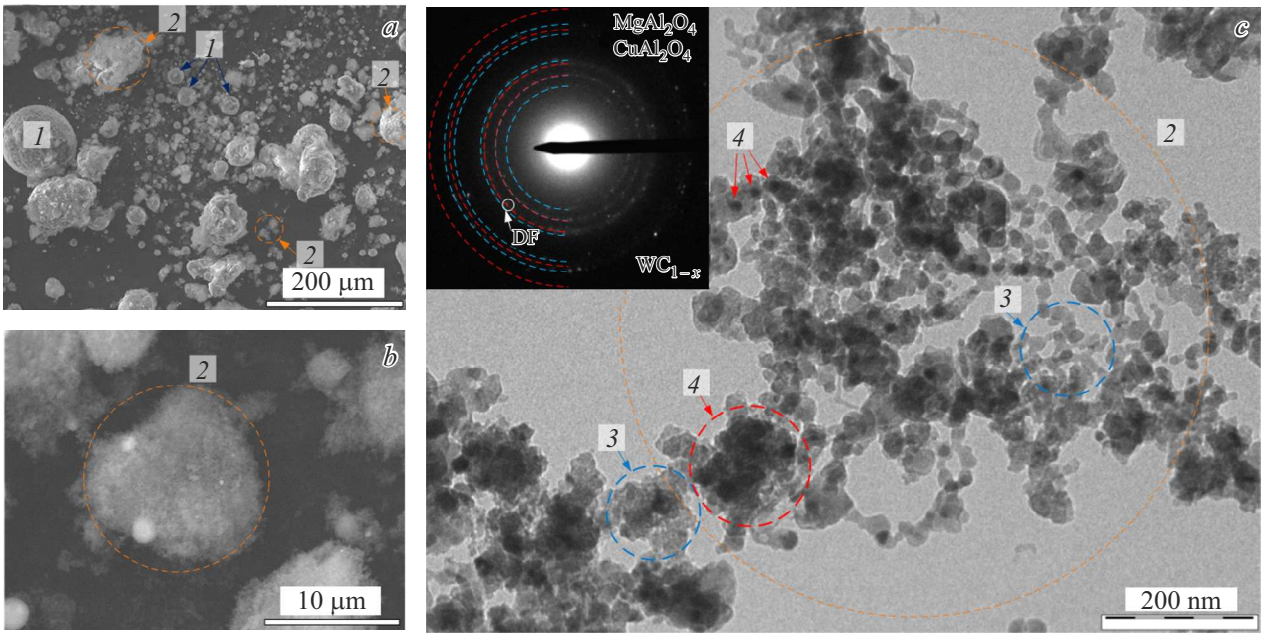

Figure 2. a, b — SEM images of the main-chamber synthesized product; c — TEM image of the buffer-chamber product; the inset presents the relevant electron-diffraction pattern.

is primarily exposed to the high-energy plasma jet which induces its erosion and sublimation into the liquid-phase state. After that, being under dynamic cooling conditions, the film crystallizes in the nanoscale state with formation of spinels contained first of all in the buffer-chamber product in the amount of ~ 26 mass%. Thereat, the presence of aluminum oxide phases was not revealed in the product.

Second, the product contains derivatives of tungsten and carbon introduced in the plasma structure formation channel, which are represented as WC_{1-x} and W_2C (predominantly, in the buffer-chamber product, ~ 17 mass%). Synthesis of unique cubic phase WC_{1-x} appears to be possible both in the system with metal electrodes and in the case of graphite electrodes [13], however, in this case the product contains also W_2C, which is caused by a slight decrease in the $p-T$ parameters in metal plasma. Both phases (WC_{1-x} and W_2C) are superhard ($H > 20$ GPa) and may be used as reinforcing additives to the finished metal-matrix item. In addition, under the plasma jet high-temperature conditions, aluminum and tungsten interact with formation of relevant tungsten aluminides of different stoichiometries ($Al_{12}W$, Al_5W and Al_4W) with the total content of 3–5 mass%; this becomes possible when concentration of W atoms exceeds its maximum solubility in liquid aluminum.

Fig. 2 presents the results of examining the products by scanning electron microscopy (SEM) (Quanta 200 3D) and transmission electron microscopy (TEM) (Philips CM12). The main-chamber product contains large sphere-like objects *1* (Fig. 2, *a*) which are, in fact, sintered micron-sized grains and clusters of highly dispersed particles *2* (Fig. 2, *b*) which are also included in the buffer-chamber product. The first type of objects may be unambiguously identified with aluminum by analogy with other metallic systems [12]. As the bright-field micrograph shows (Fig. 2, *c*), the highly dispersed fraction consists of nanoparticles *3* up to 20 nm in size, which, according to the electron diffraction pattern, belong predominantly to spinels ($MgAl_2O_4$ and $CuAl_2O_4$). More contrasting nanoparticles *4* of the cluster may be related to high-density tungsten carbides WC_{1-x}, W_2C and a number of tungsten aluminides Al_xW. This is confirmed by the dark-field TEM image of the synthesized product, which was obtained in the light of reflections 200 of crystalline phase WC_{1-x} (designated in the electron diffraction pattern as DF) and is presented jointly with the relevant bright-field image (Fig. 3). The dark-field image (Fig. 3, *b*) demonstrates glowing of reflecting planes of the considered particles contrasting in the bright-field image (Fig. 3, *a*), which is consistent with the initial assumption that they belong to tungsten-containing high-density formations (cubic tungsten carbide WC_{1-x} among them).

Thus, the paper demonstrates the possibility of forming in high-speed arc-discharge plasma the Al/Cu–Mg–W–C composite containing nanoparticles of the metastable WC_{1-x} phase. The synthesized material is suitable for producing on its base bulk metal-matrix products reinforced with superhard compounds.

Funding

The study was supported by the Russian Science Foundation, project № 23-73-01203 (https://rscf.ru/project/23-73-01203/).

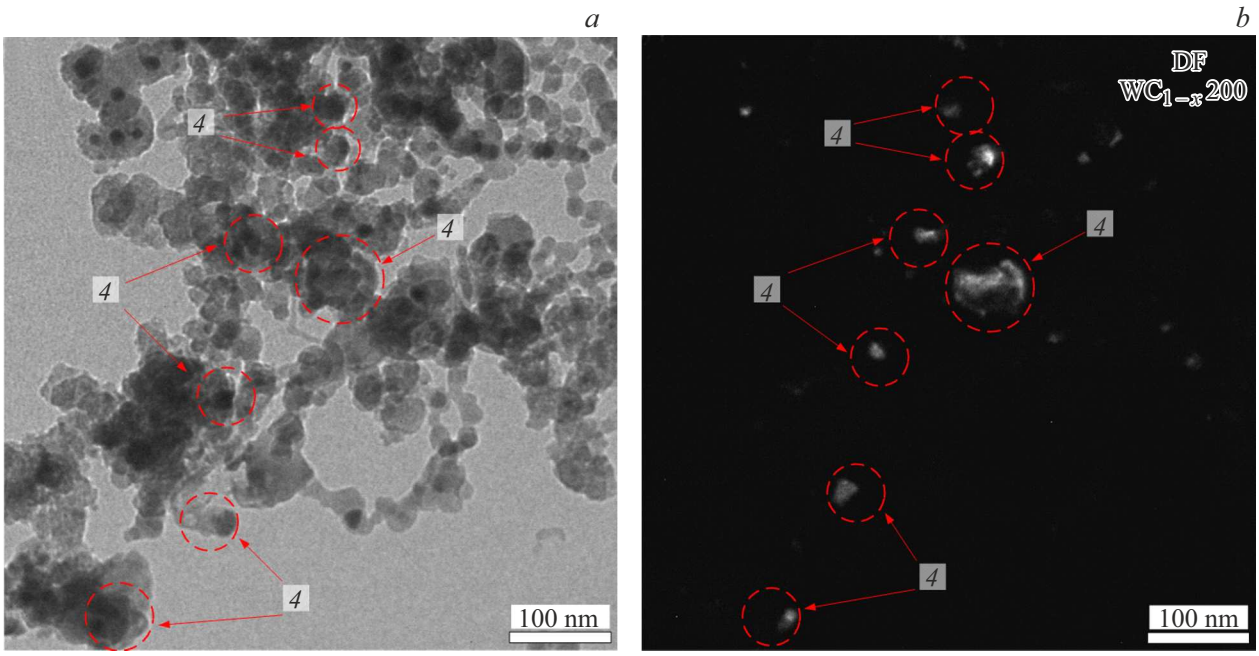

Figure 3. TEM images of the buffer-chamber synthesized product. *a* —bright-field image, *b* — relevant dark-field image in the light of 200 WC_{1-x} reflectors.

Conflict of interest

The authors declare that they have no conflict of interests.

References

[1] V.K. Parikh, V. Patel, D.P. Pandya, J. Andersson, Heliyon, **9**, e13558 (2023). DOI: 10.1016/J.HELIYON.2023.E13558
[2] M.Y. Khalid, R. Umer, K.A. Khan, Results Eng., **20**, 101372 (2023). DOI: 10.1016/J.RINENG.2023.101372
[3] D. Zhang, Prog. Mater. Sci., **123**, 100853 (2022). DOI: 10.1016/J.PMATSCI.2021.100853
[4] Z. Zhao, P. Bai, W. Du, B. Liu, D. Pan, R. Das, C. Liu, Z. Guo, Carbon, **170**, 302 (2020). DOI: 10.1016/J.CARBON.2020.08.040
[5] V. Chak, H. Chattopadhyay, T.L. Dora, J. Manuf. Process, **56**, 1059 (2020). DOI: 10.1016/J.JMAPRO.2020.05.042
[6] D.G. Kvashnin, M.K. Kutzhanov, Sh. Korte, E.M. Prikhod'ko, A.T. Matveev, P.B. Sorokin, D.V. Shtanskii, Tech. Phys. Lett., **46**, 342 (2020). DOI: 10.1134/S1063785020040094.
[7] A.A. Megahed, M.A. Mohamed, M. Abdel Hamid, S.H. Zoalfakar, Proc. Inst. Mech. Eng. C, **236**, 9148 (2022). DOI: 10.1177/09544062221091904
[8] A.R. Krishna, A. Arun, D. Unnikrishnan, K.V. Shankar, Mater. Today Proc., **5**, 12349 (2018). DOI: 10.1016/J.MATPR.2018.02.213
[9] M.Y. Zhou, L.B. Ren, L.L. Fan, Y.W.X. Zhang, T.H. Lu, G.F. Quan, M. Gupta, J. Alloys Compd., **838**, 155274 (2020). DOI: 10.1016/J.JALLCOM.2020.155274
[10] S.A. Kareem, J.U. Anaele, E.O. Aikulola, T.A. Adewole, M.O. Bodunrin, K.K. Alaneme, J. Alloys Metallurg. Syst., **5**, 100057 (2024). DOI: 10.1016/J.JALMES.2024.100057
[11] A.T. Oyewo, O.O. Oluwole, O.O. Ajide, T.E. Omoniyi, M. Hussain, Hybrid Adv., **5**, 100117 (2024). DOI: 10.1016/J.HYBADV.2023.100117
[12] I. Shanenkov, A. Tsimmerman, A. Nassyrbayev, D. Nikitin, R. Tabakaev, A. Sivkov, Ceram. Int., **49**, 34232 (2023). DOI: 10.1016/J.CERAMINT.2023.08.137
[13] I. Shanenkov, D. Nikitin, A. Ivashutenko, Y. Shanenkova, Y. Vympina, D. Butenko, W. Han, A. Sivkov, Ceram. Int., **47**, 6884 (2021). DOI: 10.1016/J.CERAMINT.2020.11.035
[14] L. Song, T.C. Zhang, Y. Zhang, B.C. Chen, M. Wu, S.Q. Zhou, Z. Mei, Mater. Today Commun., **35**, 106180 (2023). DOI: 10.1016/J.MTCOMM.2023.106180

Translated by EgoTranslating